Available online at www.sciencedirect.com
SCIENCE DIRECT®
Journal of Power Sources 141 (2005) 286–292
JOURNAL OF POWER SOURCES
www.elsevier.com/locate/jpowsour

Multilayered Sn–Zn–Cu alloy thin-film as negative electrodes for advanced lithium-ion batteries

Lianbang Wang[a,1], Shingo Kitamura[b], Keigo Obata[b], Shigeo Tanase[a], Tetsuo Sakai[a,*]

[a] *National Institute of Advanced Industrial Science and Technology (AIST), Kansai Center, 1-8-31, Midorigaoka, Ikeda, Osaka 563-8577, Japan*
[b] *R&D Center, Daiwa Fine Chemicals Co., Ltd., 21-8, Minamifutami, Futami-cho, Akashi, Hyogo 674-0093, Japan*

Received 17 March 2004; received in revised form 5 July 2004; accepted 1 October 2004
Available online 26 November 2004

Abstract

Sn-based alloy compounds have been considered as possible alternatives for carbon in lithium-ion batteries and attract great attentions because of their large electrochemical capacity compared with that of carbon. In this work, a multilayered Sn–Zn/Zn/Cu alloy thin-film electrode has been prepared by electroplating method. The structure and performance of the electrode before and after heat treatment have been investigated. It is found that Cu_6Sn_5 phase and multilayered structure in electrode are formed after heat treatment. This optimized structure of the heat-treated electrode results in enhanced cycle life. The capacity of the electrode is over 320 mA h g^{-1} after 100 cycles; though it is 83 mA h g^{-1} after 20 cycles for as-plated electrode. The Sn–Cu and Zn–Cu alloy formed a network in the electrode is considered to strengthen the electrode and reduce the effect of volume expansion and phase transition during cycling. Experimental results also reveal that lower cut-off potential (0.05 V) for charging and higher one (1.2 V) for discharging result in long cycle life and high discharge capacity, respectively. The reason of capacity decay of the heat-treatment electrode during cycling has also been investigated. All these results show that the electroplated Sn–Zn-based alloy film on Cu foil would be a promising negative material with high capacity and low cost for Li secondary batteries.

Keywords: Li-ion batteries; Electroplating method; Multilayered Sn–Zn–Cu alloy thin-film electrode; Heat treatment

1. Introduction

Lithium-ion batteries are widely being used as the power sources for modern consumer electronic devices, such as mobile phones and notebook computers. Carbon is normally used as negative materials in commercial Li-ion batteries. In order to increase the energy density and specific energy of such batteries, intense research activity is aimed at the development of new electrode materials. Sn-based alloy compounds have been considered as possible alternatives for graphite in Li-ion batteries and attract great attention because of large electrochemical capacity (990 mA h g^{-1}), compared with that of carbon (372 mA h g^{-1}). However, large volume and structure changes occur associated with the reversible reaction of Li-insertion and extraction, which result in severe cracking of active material in electrode and loss of electrical contact [1]. It is believed that particle cracking of electrode resulting from volume expansion and phase transition is responsible for the poor cycle performance of Sn-based alloy electrode [2]. This prevents the widespread use of such alloys in Li-ion batteries.

Many attempts have been done for the aim of application of Sn-based alloy electrode in Li-ion secondary batteries and significant developments have been obtained. Successful methods include the applications of such materials as following: (1) materials with small particle size, such as nanosized SnSb [3] and Sn–Cu–B [4], nano-Sn, $Li_{4.4}Sn$ [2], nanostruc-

* Corresponding author.
E-mail addresses: Wang_lb2001@yahoo.com.cn (L. Wang), sakai-tetsuo@aist.go.jp (T. Sakai).
[1] Present address: Zhejiang University of Technology, China. Tel.: +86 571 8832 0813; fax: +86 571 8832 0813.

0378-7753/$ – see front matter © 2004 Elsevier B.V. All rights reserved.
doi:10.1016/j.jpowsour.2004.10.006

ture Sn oxide [5,6], nanocrystalline Ni_3Sn_4 [7]; (2) intermetallic compounds [8], such as η'-Cu_6Sn_5 [9], flake Sn–Cu alloy [10], Cu_6Sn_x ($x = 4, 5, 6$) [11], Sn–Mn–C [12]; (3) composites, such as multiphase metallic $Sn/SnSb_n$, $Sn/SnAg_n$ [13], C–Sn composite [14,15], Sn oxide composites [16]; and (4) thin-film, such as electroplated Sn, Cu–Sn [17] and $SnZr_x$ alloy [18].

In our research group, electroplating method was used to prepare Sn [19–21] and Sn–Zn alloy thin-film electrodes [22,23], and then heat treatment was applied to form Cu_6Sn_5 intermetallic alloy, which resulted in remarkable improvement in discharge capacity and cycle life.

Based on previous studies [24], we found that the main reason of capacity decay of Sn-based thin-film electrode was that active material cracked and isolated from Cu substrate. In order to improve the performances of such electrode, we want to combine the advantages of intermetallic alloys and thin film electrode. In this work, electroplating method has been used to prepare multilayered Sn–Zn/Zn/Cu sample. The Zn layer is expected to strengthen the contact between active material and Cu substrate because metallic Zn could form a solid solution with Sn and Cu [25] without forming a stable lithiated compound. Electrochemical performances and structural changes of the sample before and after heat treatment have been investigated.

2. Experimental

Multilayered Sn–Zn/Zn/Cu thin-film alloy were prepared by electroplating Zn film, Sn–Zn alloy film on Cu foil in sequence. The electroplating conditions have been reported [21,22]. The concentration of Zn in Sn–Zn layer was around 7–15 wt.%. The thickness of plated film (Zn plus Sn–Zn) on Cu foil was around 3–6 μm. The testing electrode was punched from electroplated sample in the diameter of 1 cm. Heat treatment was carried out under vacuum at the temperature range of 180–230 °C in order to improve the performance of the electrode.

Testing cells were assembled by using the Sn–Zn/Zn/Cu alloy electrode as working electrode, and Li sheet as counter electrode. The electrolyte was 1M $LiPF_6$ in EC:DMC (1:2 by volume ratio). Assembly of cells was carried out in drying room. Current densities for charging (Li insertion) and discharging (Li extraction) were 0.2 mA cm^{-2} for the first activation cycle and after that were 0.4 mA cm^{-2} and 1.0 mA cm^{-2}, respectively. The potential range of charge-discharge was 0–1.0 V versus Li/Li^+. Various cut-off potentials have also been examined to obtain suitable cut-off potential.

Crystal structures of electrodes were characterized by X-ray diffraction analysis (XRD) using a $M06X^{CE}$ diffractometer with CuK_α radiation source (MAC Science, Co. Ltd.). In order to avoid the oxidation of electrode samples, a specially designed airtight X-ray sample holder was used. The electrolyte on the surface of the electrode after cycling was not removed when the XRD experiment was carried out. Microstructure of electrodes was examined by scanning electron microscopy (SEM) (S-2150, HITACHI, Ltd.) with energy dispersion X-ray spectroscopy (EDXS) (EMAX-7000, HORIBA, Ltd.). The electrodes after cycling for SEM experiment should be washed carefully by PC and dehydrated acetone in sequence, then dried under vacuum at ambient temperature. The fine structure of electrode at full Li-insertion has been examined by a high-resolution transmission electron microscopy (HRTEM) (JOEL JEM-3010) with Pt sputter coater using FEI-200 (FEI, Japan).

3. Results and discussion

3.1. Cyclic behaviors of multilayered Sn–Zn/Zn/Cu electrode

Fig. 1 shows the cyclic behaviors of Sn–Zn/Zn/Cu alloy electrode before and after heat treatment. As-plated electrode shows high discharge capacity at initial 10 cycles, over 660 mA h g^{-1}, twice as that of carbon. But, at the following 10 cycles, the discharge capacity of the as-plated electrode decays severely from 660–83 mA h g^{-1} due to the loss of contact between plated film and Cu foil, resulted from the change of volume and phase transition during cycling.

After heat treatment, it is clear that the cyclic durability of electrode has been improved remarkably. The electrode after heat treatment shows the discharge capacity, 321 mA h g^{-1} after 100 cycles and 120 mA h g^{-1} after 200 cycles, respectively. In order to determine the remarkable change of charge–discharge cyclic durability of the electrodes before and after the heat treatment, the structure change of the electrode caused by heat treatment has been investigated.

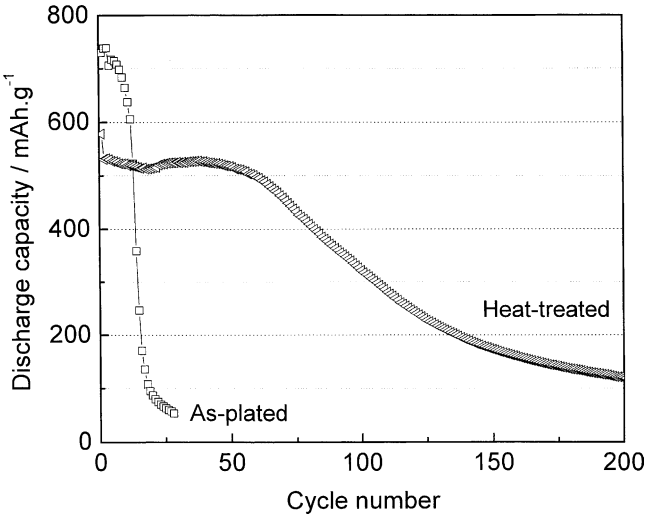

Fig. 1. The discharge cyclic behaviors of multilayered Sn–Zn/Zn/Cu thin-film electrodes before and after heat treatment.

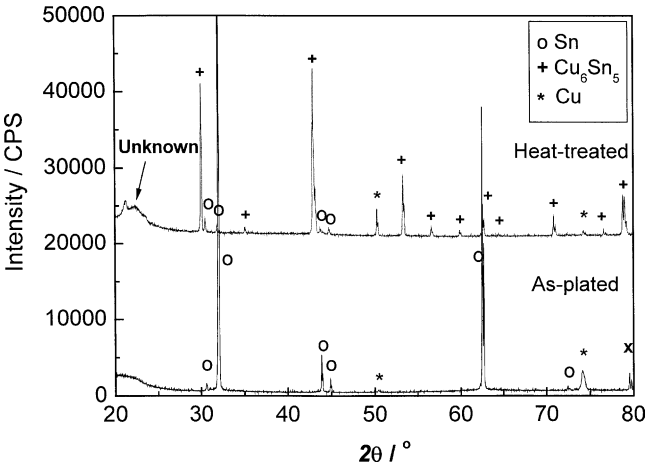

Fig. 2. XRD patterns of multilayered Sn–Zn/Zn/Cu thin-film electrodes before and after heat treatment.

3.2. Effect of electrode structure on the cyclic behaviors

Fig. 2 presents the XRD patterns of the Sn–Zn/Zn/Cu alloy electrode before and after the heat treatment. The result shows that the as-plated electrode is composed of plated Sn phase and Cu foil. The content of Zn is too low to be observed in XRD patterns. After heat treatment, Cu_6Sn_5 phase was formed in the plated film of the electrode, but a small amount of metallic Sn were still remained in the electrode.

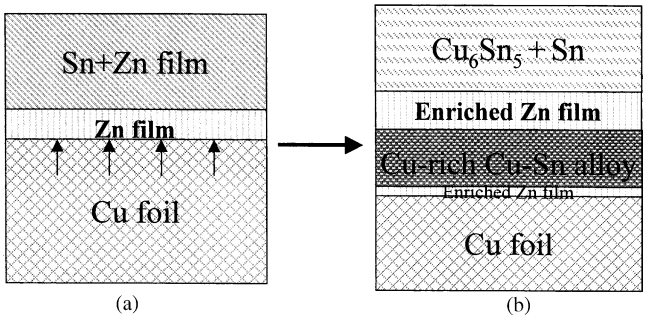

Fig. 4. Structure change model of multilayered Sn–Zn/Zn/Cu thin-film electrodes during heat treatment under vacuum.

SEM–EDXS spectra of the cross-section of electrodes before and after the heat treatment have been shown in Fig. 3. These figures clearly show the diffusing behavior of Zn layer and Cu foil. The Cu diffuses from the Cu foil to the surface of the electrode, and the concentration of Cu increases gradually from the surface to the substrate. The Zn film is separated into two parts.

Based on the results of Figs. 2 and 3, we give the structural model of the electrode before and after heat treatment

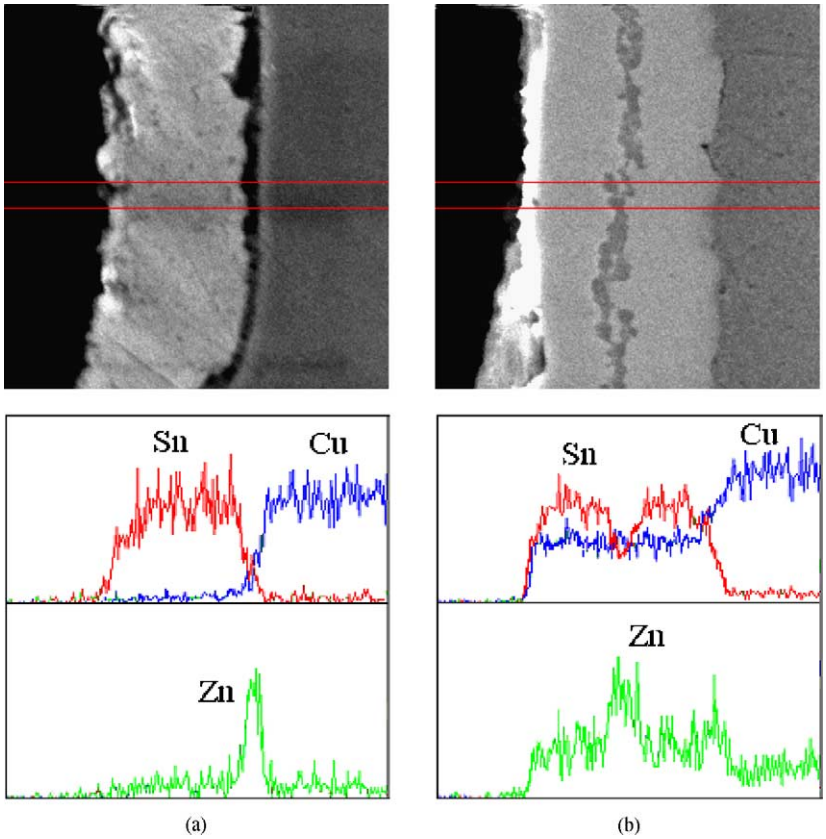

Fig. 3. SEM–EDXS images of cross-section of electrodes before and after heat treatment.

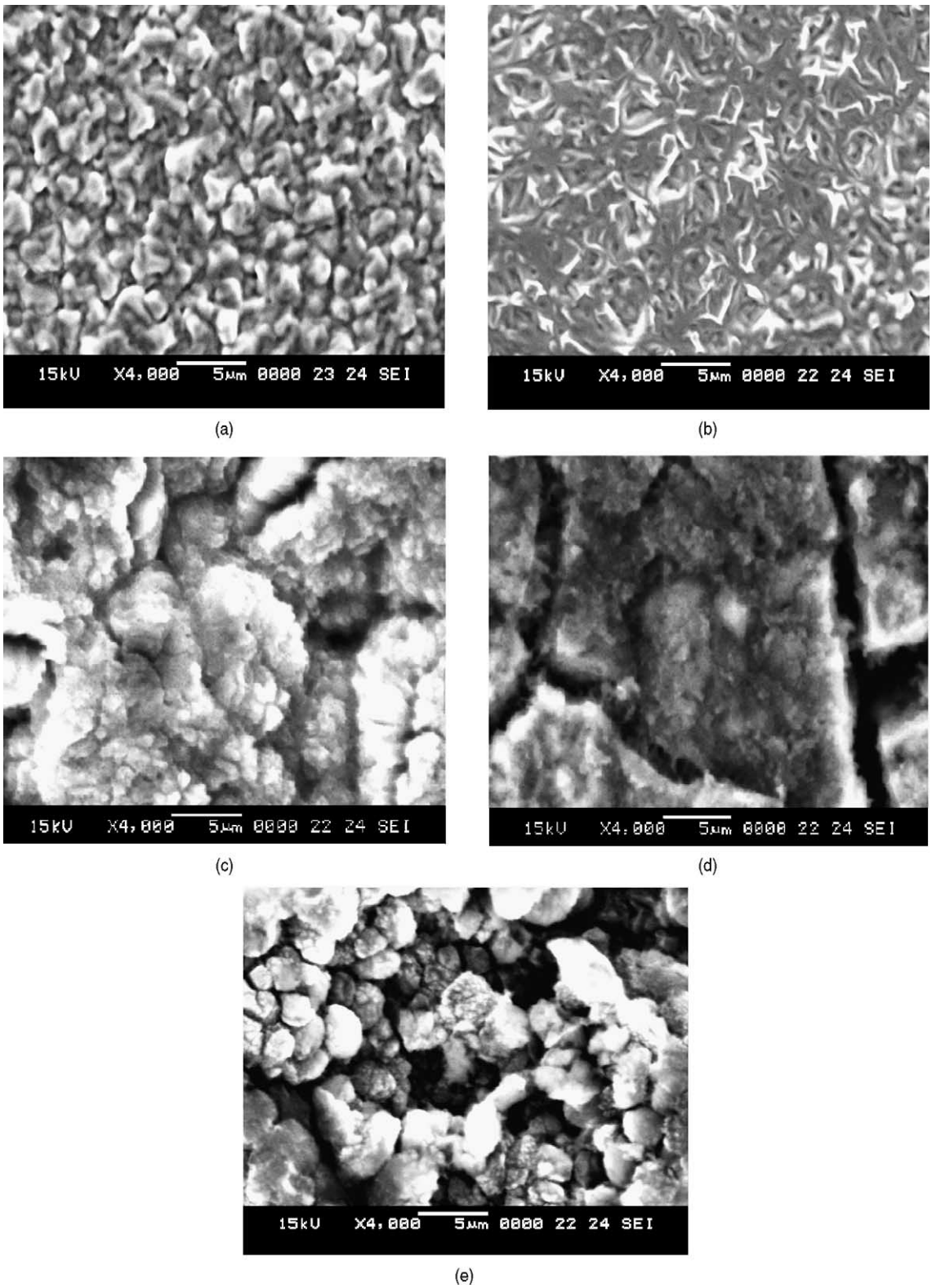

Fig. 5. The surface microstructure of electrodes: (a) as-plated; (b) after heat-treated; (c) after 1 cycle; (d) after 10 cycles; (e) after 100 cycles. The cut-off potential of electrode after cycling is 0 V (full Li-insertion) vs. Li/Li^+ electrode.

as presented in Fig. 4. The as-plated electrode (Fig. 4a) is composed of three layers, electroplated Sn–Zn film layer and Zn film layer, and Cu substrate layer. During the heat treatment, the Zn film was separated into two parts because of the diffusion of Cu from the Cu foil towards the surface of the electrode. The Cu diffusing from the Cu substrate to the surface of the electrode took the Zn layer moving into the bulk of the plated Sn–Zn layer, and only a very thin Zn film was still remained at the interface between plated film and Cu foil (Fig. 4b). At the same time, Cu_6Sn_5 phase was formed in active material layer. After this process, the contact between electroplated layer and Cu foil was strengthened. On the surface of the electrode, a small amount of metallic Sn was still remained due to the absence of Cu.

These results revealed that the cycle life and discharge capacity of the heat-treated Sn–Zn/Zn/Cu alloy electrode was improved remarkably because of the formation of Cu_6Sn_5 phase and multilayered structure. The Cu_6Sn_5 intermetallic phase as active material in the plated film reacted with inserted Li to form $Li_{22}Sn_5$ compound and metal Cu. The decomposed Cu was used as matrix and binder to relax the volume expansion. At the same time, the two Zn layers, which did not form stable lithiated compounds with inserted Li, strengthened the contact between the active material layer and the Cu foil. All the factors resulted in the remarkable improvement of the cycle life of the electrode after the heat treatment.

3.3. Structure change of electrode during charge-discharge process

Fig. 5a–e shows the surface images of the electrodes. The surface of as-plated electrode was composed of electroplated alloy particles (Fig. 5a). After heat treatment, Cu_6Sn_5 intermetallic phase was formed, and the surface of the electrode looked like wrinkles (Fig. 5b). In the first Li-insertion process, cracks emerged on the surface of the electrode due to the large volume expansion and phase transition, which was associated with the formation of $Li_{4.4}Sn$ compounds (Fig. 5c). The thickness of the electrode increased from 24 μm to 36 μm after first Li-insertion. With the increase of cycles, cracks became larger and larger (Fig. 5d); the active material in the plated film of electrode broke into fine particles after 100 cycles (Fig. 5e). These results reveal that the particles of active material cracked gradually during cycling, which resulted in the loss of contact between them, and the plated film was isolated or peeled from the Cu foil, so the discharge capacity of the electrode decayed. The formation of the Cu_6Sn_5 intermetallic phase relaxed the cracking process to a certain degree and improved the cycle life of the electrode.

Fig. 6 shows the HRTEM image of the heat-treated Sn–Zn/Zn/Cu thin-film electrode after full Li-insertion at the initial cycle. Point 1 was composed of 64.45%-Sn atom, 0.94%-Zn atom and 34.61%-Cu atom; it was compatible with the XRD results, Sn-riched Sn–Cu alloy. Point 2 was

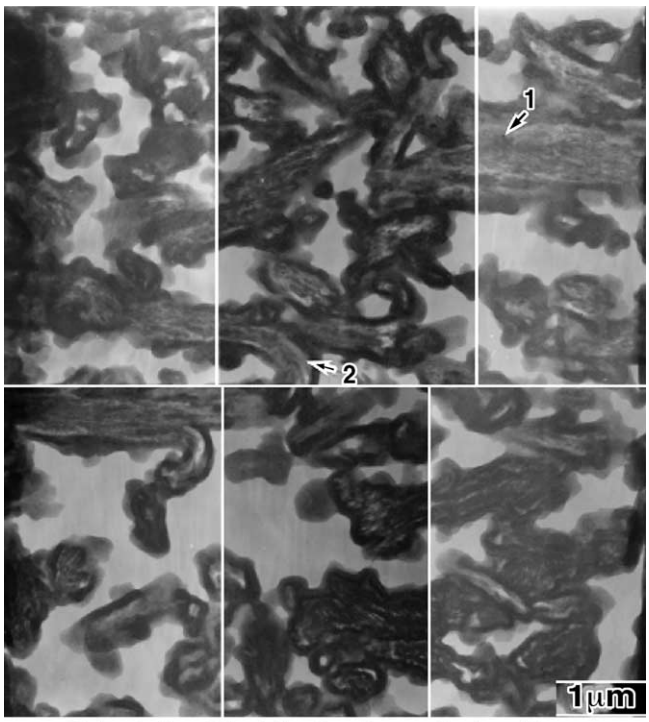

Point 1: Sn-riched Sn-Cu alloy and minor Zn
Point 2: Zn-Cu alloy

Fig. 6. HRTEM image of electrode after full Li-insertion at initial charging process. Current density: 0.2 mA h cm^{-2}, cut-off potential: 0 V vs. Li/Li^+ electrode.

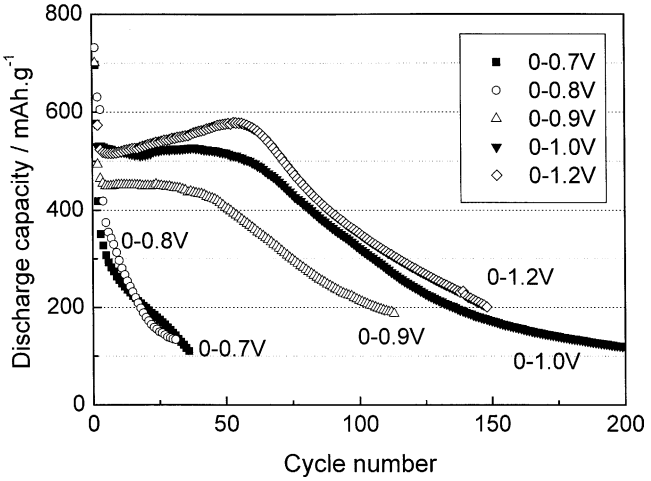

Fig. 7. Cyclic behaviors of electrodes at various cut-off potentials for discharging (Li-extraction).

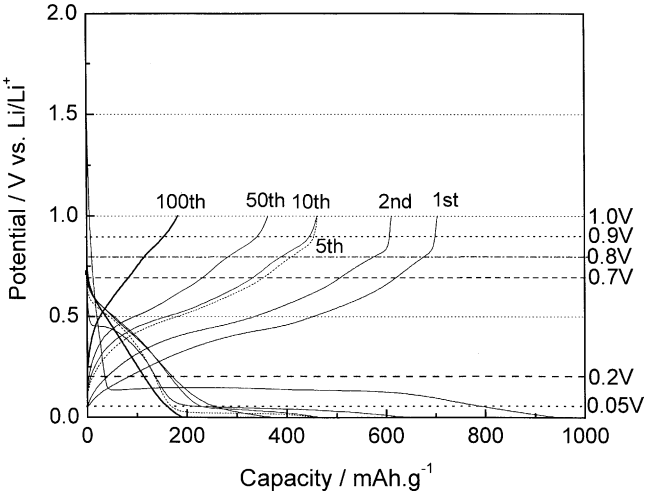

Fig. 9. The charge–discharge curves of the multilayered Sn–Zn/Zn/Cu alloy thin-film electrode after heat treatment.

composed of 68.90%-Zn atom and 31.10%-Cu atom; the ratio was compatible with $CuZn_2$ alloy. The content of Zn–Cu alloy in the electrode may be too low to be observed in XRD patterns. The transparent area of the image could be $Li_{4.4}Sn$ compound. This TEM image clearly shows that a Sn–Cu and Zn–Cu alloy network was formed in the plated film of the electrode. The network could relax the volume expansion during cycling, which could explain why the cycle life of the electrode was remarkably improved after heat treatment.

3.4. Effect of cut-off potential on the cyclic behaviors

Figs. 7 and 8 shows the cyclic behaviors of the electrodes at various cut-off potentials. Fig. 7 presents the cyclic behaviors of the electrodes at various cut-off potentials for discharging, from 0 V to 0.7, 0.8, 0.9, 1.0, and 1.2 V versus Li/Li^+, respectively. At the cut-off potentials of 0.7 and 0.8 V, part of the inserted Li in the electrode could not be discharged, but accumulated during cycling, which resulted in the loss of discharge capacity as shown in Fig. 9. The discharge capacity of the electrode decreased quickly. At the high cut-off potentials of 1.0 V and 1.2 V, the inserted Li could be extracted sufficiently, which resulted in the high discharge capacity. At the potential of 0.9 V, the discharge capacity of the electrode was lower than that at 1.0 V and 1.2 V, but higher than that at 0.7 V and 0.8 V. These results suggest that the cut-off potential of the electrode should be over 1.0 V to obtain high discharge capacity.

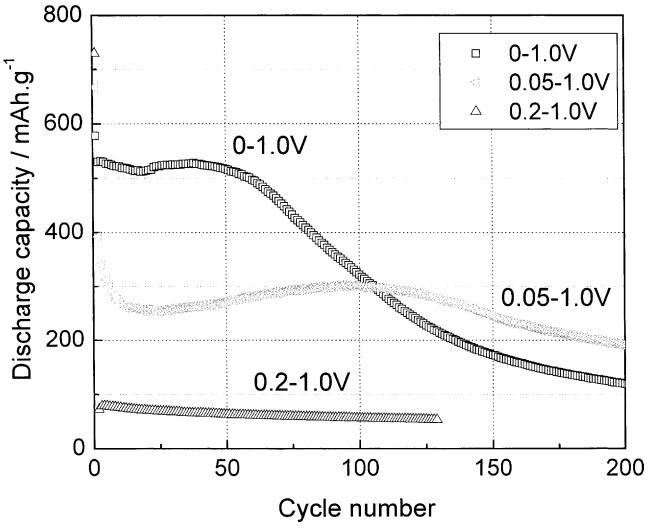

Fig. 8. Cyclic behaviors of electrodes at various cut-off potentials for charging (Li-insertion).

Fig. 8 shows the cyclic behaviors of the electrodes at various cut-off potentials for charging, from 0, 0.05 and 0.2 V to 1.0 versus Li/Li^+, respectively. The cut-off potential of 0.2 V was much higher than Li-inserted plateau potential around 0.04 V shown in Fig. 9. It means that the Li cannot be inserted into the active material in the electrode; most of the active material cannot be used, which results in the lower rechargeable capacity. The cut-off potential of 0.05 V was still a little higher than the main Li-inserted plateau around 0.04 V. From our previous report [22], the reaction plateau around 0.04 V was associated with the phase conversion from $CuLi_2Sn$ to $Li_{4.4}Sn$. At the higher cut-off potential over 0.04 V, the formation of $Li_{4.4}Sn$ was limited strictly, which resulted in low capacity, but long cycle life. The discharge capacity of electrode at the cut-off potential of 0.05 V was 193 mA h g^{-1} (1404 mA h/cc-SnZn) even after 200 cycles. The volumetric capacity of the electrode was much higher than that of carbon material for Li-ion batteries. These results suggest that conscious controlling of the cut-off potential window is one of the approaches to improve the cycle life of the electrode efficiently.

4. Conclusions

In this work, electroplating method has been used to prepare multilayered Sn–Zn/Zn/Cu alloy film electrode for

advanced Li-ion batteries. It is found that the discharge capacity and the cycle life of electrode were improved remarkably by heat treatment because of the formation of Cu_6Sn_5 intermetallic phase and multilayered electrode structure. The discharge capacity of the heat-treated electrode was maintained over 320 mA h g^{-1} after 100 cycles; however, it was only 83 mA h g^{-1} after 20 cycles for the as-plated electrode. A Sn–Cu and Zn–Cu alloy network formed in the electrode could enhance the mechanical strength and relax the volume expansion of the electrode, resulting in the enhanced cyclic durability. During cycling, the active material layer was cracked gradually, which resulted in the loss of the contact between alloy particles and the decay of the discharge capacity and the cyclic durability. Conscious controlling of the cut-off potential window is one of the approaches to obtain high discharge capacity and good cyclic durability of the electrode. The electroplated Sn–Zn-based alloy film on Cu foil could be a promising negative material for Li-ion secondary batteries through further improvement in the cyclic durability.

Acknowledgement

This study is a part of “Regional Consortium Research Development Work” supported by METI.

References

[1] M. Winter, J.O. Besenhard, Electrochim. Acta 45 (1999) 31.
[2] C. Wang, A.J. Appleby, F.E. Little, J. Power Sources 93 (2001) 174.
[3] H. Li, L.H. Shi, W. Lu, X.J. Huang, L.Q. Chen, J. Electrochem. Soc. 148 (2001) A915.
[4] D.G. Kim, H. Kim, H.-J. Sohn, T. Kang, J. Power Sources 104 (2002) 221.
[5] N. Li, C.R. Martin, B. Scrosati, J. Power Sources 97/98 (2001) 240.
[6] N. Li, C.R. Martin, J. Electrochem. Soc. 148 (2001) A164.
[7] H.Y. Lee, S.W. Jang, S.M. Lee, S.J. Lee, H.K. Baik, J. Power Sources 112 (2002) 8.
[8] R. Benedek, M.M. Thackeray, J. Power Sources 110 (2002) 406.
[9] D. Larcher, L.Y. Beaulieu, D.D. MacNeil, J.R. Dahn, J. Electrochem. Soc. 147 (2000) 1658.
[10] Y.Y. Xia, T. Sakai, T. Fujieda, M. Wada, H. Yoshinaga, J. Electrochem. Soc. 148 (2001) A471.
[11] K.D. Kepler, J.T. Vaughey, M.M. Thackeray, J. Power Sources 81/82 (1999) 383.
[12] L.Y. Beaulieu, J.R. Dahn, J. Electrochem. Soc. 147 (2000) 3237.
[13] J. Yang, M. Winter, J.O. Besenhard, Solid State Ionics 90 (1996) 281.
[14] G.X. Wang, A. Jung-Ho, M.J. Lindsay, L. Sun, D.H. Bradhurst, S.X. Dou, H.K Liu, J. Power Sources 97/98 (2001) 211.
[15] M. Egashira, H. Takatsuji, S. Okada, J.I. Yamaki, J. Power Sources 107 (2002) 56.
[16] L.A. Courtney, J.R. Dahn, J. Electrochem. Soc. 144 (1997) 2045.
[17] N. Tamura, R. Ohshita, M. Fujimoto, S. Fujitani, M. Kamino, I. Yonezu, J. Power Sources 107 (2002) 48.
[18] S.J. Lee, H.Y. Lee, S.H. Jeong, H.K. Baik, S.M. Lee, J. Power Sources 111 (2002) 345.
[19] T. Sonada, T. Fujieda, T. Sakai, The 41st Battery Symposium in Japan, 2000, p. 532.
[20] T. Sonoda, Battery Technol. 14 (2002) 14.
[21] S. Kitamura, D. Kim, M. Yoshimoto, K. Obata, T. Sonoda, T. Sakai, The 42nd Battery Symposium in Japan, 2001, p. 288.
[22] L. Wang, S. Kitamura, T. Sonoda, K. Obata, S. Tanase, T. Sakai, J. Electrochem. Soc. 150 (10) (2003) A1346–A1350.
[23] S. Kitamura, L.B. Wang, S. Tanase, K. Obata, T. Sakai, Electrochemistry 12 (2003) 1070–1072.
[24] L.B. Wang, S. Kitamura, T. Sonoda, D.H. Kim, K. Obata, S. Tanase, T. Sakai, The 43rd Battery Symposium in Japan, 2002, p. 26.
[25] T.B. Massalski, Binary Alloy Phase Diagram, William W. Scott, 1986, p. 2086.